Transport Phenomena in Bottom Blown Bath by O_2, CO_2, CO, Ar, N_2, H_2O, H_2 and Gas Mixture

HAIPING SUN, YUNG-CHANG LIU and MUH-JUNG LU

Iron and Steel Research & Development Department
China Steel Corporation

A mass and heat transport model for a multicomponent bubble in metal was developed by coupling the rates and thermal effects of reactions and the mass and heat transport between metal and gas. The physical, chemical, mass transport and energy transport phenomena in a high carbon bath injected from the bottom with eight different gases were investigated and compared by the model.

Keywords: Steelmaking, Steel refining, Bottom blowing, Bubble, Mass and heat transport

1. INTRODUCTION

In many steelmaking and steel refining processes, gas or a gas mixture is injected into the bath from the bottom for heating, removing impurities, degassing, cooling refractory and/or stirring. The injected gas must be suitable for the production of the steel of a required composition during a given time period in a specific injection process. Many laboratory scale studies have been carried out on the gas bubble characteristics in the molten iron,[1] absorption/desorption of oxygen,[2] nitrogen,[3] hydrogen[4] and decarburization[5-8] in metal by gas or gas mixture, and heat transfer between gas bubble and metal.[9,10] Based on these studies, the physical, chemical and thermal histories of an oxygen bubble during the bottom blown process were investigated.[11] To further extend our understanding, a mass and heat transport model for a multicomponent bubble in metal was developed in this study. The model, coupling multiple heterogeneous and homogeneous reactions, is the first of its kind for the revelation of histories of different types of gas in the bottom blown process.

2. DESCRIPTION

When a bath is injected with gas from the bottom, the gas disperses into bubbles and rises in the bath. The bubbles were observed to be close to spherical[1] due to the larger surface tension of the steel. The bubbles react and exchange heat with the surrounding metal until they reach the surface of the bath. During their path towards the bath surface, the bubbles' size changes with the changes in pressure, number of moles and temperature of the bubbles according to the idea gas law. The pressures on the bubbles changes with ambient, hydrostatic and Laplace pressures. The number of moles and the composition of the bubbles are changed by the reactions of the bubbles with metal. The temperature of the bubbles also changes due to the thermal effects of these reactions and the heat exchange between the bubbles and the surrounding metal. The rising velocity of a bubble is the Stokesian velocity in addition to the velocity of the circulation flow in the bath. Stokesian velocity changes with the bubble size but the velocity of the circulation flow does not change during a bubble's life.

3. MASS TRANSPORT

The mass transport between the metal and the gas bubble are schematically shown in Fig.1. If the gas in a bubble is a mixture of O_2-CO_2-CO-Ar-N_2-H_2O-H_2 and the metal in a bath is a mixture of Fe-C-O-N-H, reactions (1)-(6) may occur at gas-metal interface and reactions (7) and (8) may occur in the gas.

$$O_2 = 2\underline{O}^{ex} \quad (1)$$

$$CO_2 = \underline{O} + CO^{en} \quad (2)$$

$$\underline{C} + \underline{O} = CO^{ex} \quad (3)$$

$$N_2 = 2\underline{N}^{en} \quad (4)$$

$$H_2O = \underline{O} + H_2^{en} \quad (5)$$

$$H_2 = 2\underline{H}^{en} \quad (6)$$

$$O_2 + 2CO = 2CO_2^{ex} \quad (7)$$

$$CO + H_2O = CO_2 + H_2^{ex} \quad (8)$$

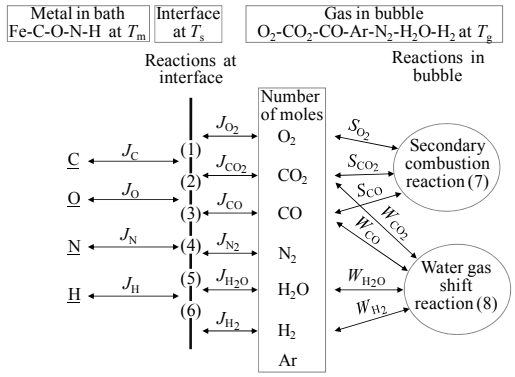

Fig.1. Mass transport between metal and gas bubble.

According to the enthalpy[12-14] changes of reactions at 1500 °C, the reactions superscripted with "ex" are exothermic and those with "en" are endothermic. Many combined reactions can be derived from the independent reactions (1) through (8). The combined reactions are not included in the development of the model. Instead, they were referred to when interpreting the modeling results.

Due to the reactions (1) through (6) at the gas-metal interface, some species are reactants which migrate from gas or metal into the interface, while others are products which migrate out of the interface into gas or metal. As indicated by J_i in Fig.1, the migration rate of a species in gas or in metal down the concentration gradient into or out of the interface are given by a two-film theory as

$$J_i = k_i\left(c_i - c_i^*\right)$$

(i=C, O, N, H, O_2, CO_2, CO, N_2, H_2O or H_2)

..... (9)

The mass transfer coefficients (k_i) in the boundary layer at both sides of the interface are estimated by a mass transfer coefficient model suggested by Mori *et al.*[2] according to the surface renew model[15] for a bubble rising in relation to metal. The Stokesian velocity[16] and diffusivities of species in metal[17] and in gas[18] were used in the estimation. The viscosity and density of metal[19] was used to estimate the Stokesian velocity from the bubble size. The rates of the reactions at the interface for carbon,[5-8] hydrogen[4] and oxygen[2] are suggested to be dominated by the migration rate in gas and/or in metal given in Equation (9). In addition to being dominated by the migration rate, the reaction (4) at the gas-metal interface was reported[3] to be sluggish and be affected by sulfur and oxygen contents in the metal. The rate of the reaction (4) at interface described by the mass action law[3] was taken into account in this work.

The concentrations (c_i^*) at the gas or metal side of the gas-metal interface are solved from the mass conservations of carbon, oxygen, nitrogen and hydrogen at the interface alongside (a) the equilibrium relations[20] for the reactions (1) through (6) at the gas-metal interface at T_s, (b) the content-pressure conversions for the gas species, (c) the content-activity conversions for the species in metal and (d) the activity coefficient-content conversions for the species in metal which involve the interaction parameters[16]. The solved c_i^* is, in turn, used in Equation (9) to find the migration rate of a species into, or out of, the interface.

The change in the number of moles of a gas species in a bubble is given by

$$\frac{dn_i}{dt} = -AJ_i + VS_i + VW_i$$

(i = O_2, CO_2, CO, N_2, H_2O or H_2).....(10)

At the right hand side of the above equation, the first term is the number of moles lost from gas into the gas-metal interface, the second term is those generated by the secondary combustion reaction (7) in the bubble and the last term is those by the water gas shift reaction (8) in the bubble. S_i (i = O_2, CO_2, CO) are the generation rates of O_2, CO_2 and CO by reaction (7) and W_i, (i = CO_2, CO, H_2O, H_2) are those of H_2O, CO, H_2 and CO_2 by reaction (8) in the bubble. Knowing J_i from Equation (9), S_i, W_i and dn_i/dt are able to be solved from the stoichiometry and equilibriums[12] of reactions (7) and (8) in the bubble. The variation of gas composition in the bubble is then obtained from Equation (10).

4. HEAT TRANSPORT

Fig.2 schematically shows the heat transport between the metal and the gas bubble. The sum of thermal effects of reactions (1) through (6) at the interface can be obtained by differences in the enthalpies[12-14] of the species migrating out of and those migrating into the interface as

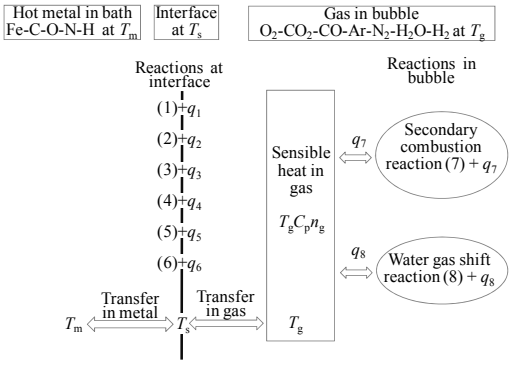

Fig.2. Heat transport between metal and gas bubble.

$$\sum_{i=1}^{6} q_i = \sum AJ_j H_j$$

(j = C, O, N, H, O_2, CO_2, CO, N_2, H_2O or H_2)

.....(11)

T_s was determined from the heat conservation at the bubble surface by

$$Ah_m(T_s - T_m) = \sum_{i=1}^{6} q_i + Ah_g(T_g - T_s)$$

.....(12)

The left hand side of the above equation is the heat transfer rate from interface at T_s into metal at T_m; it is the rate of heat supply from the gas to the bath. At the right hand side, the first term is the rate of heat provided by the reactions at the interface and the second term is heat transferred from gas bulk at T_g to the surface at T_s. The heat transfer coefficients h_m in metal or h_g in bubble were estimated from a heat transfer coefficient model[10] according to penetration theory which involves bubble size, Stokesian velocity, thermal capacities[12-14] and thermal conductivities[21] in metal or in gas.

The thermal effects of the homogenous reactions (7) and (8) in the gas phase directly changes the sensible heat of the gas. The rate of the heat provided by reaction (7) is

$$q_7 = -V\left(S_{CO_2}H_{CO_2} - S_{O_2}H_{O_2} - S_{CO}H_{CO}\right) \quad \text{..... (13)}$$

That by reaction (8) is

$$q_8 = -V\left(W_{H_2}H_{H_2} + W_{CO_2}H_{CO_2} - W_{H_2O}H_{H_2O} - W_{CO}H_{CO}\right)$$

..... (14)

The temperature in the bubble is found from the heat conservation in the bubble by

$$\frac{dT_g}{dt}\sum C_{pi}n_i = q_7 + q_8 - Ah_g(T_g - T_s)$$

(i = O_2, CO_2, CO, Ar, N_2, H_2O or H_2)..... (15)

In the above equation, the left hand side is the increase of the sensible heat of the bubble. On the right hand side, the first term is the rate of the heat provided by reaction (7); the second term is that provided by reaction (8), and the last term is that transferred from the gas bulk at T_g into the surface at T_s.

5. RESULTS AND DISCUSSION

The model developed in the previous sections was applied to a hypothetical process whereby a liquid metal bath is blown by eight different gases of O_2, CO_2, CO, Ar, N_2, H_2O, H_2 or a Mix of (25%O_2-25%CO_2-25%N_2-25%H_2O) under otherwise same process conditions as the following: a gas at 200°C is blown into a 2 m deep bath from the bottom; the gas forms numerous bubbles of 0.01 m in radius at the bath bottom before rising in the bath; the velocity of the metal circulation flow in a bath induced by bubbles in an upward direction is 1 m/s; the bath is an Fe-3C-0.0025O-0.005N-0.0005H-0.005S (in mass%) liquid at 1500°C whereby the oxygen content is in equilibrium with the carbon in the metal under ambient pressure.

After being injected at the bottom of the bath, the bubbles are carried by a buoyant force and the circulation flow in the bath to rise towards the bath surface. The residence time of the bubbles vs. height relationship as shown in Fig.3 was obtained from the velocities of Stokesian and the circulation flow in the bath. A bubble's life is the residence time of a bubble until it reaches the bath surface at 2 m above the bottom. The lives read in Fig.3 at the bath surface are in the order of H_2, N_2, CO, Ar, H_2O, Mix, CO_2, O_2.

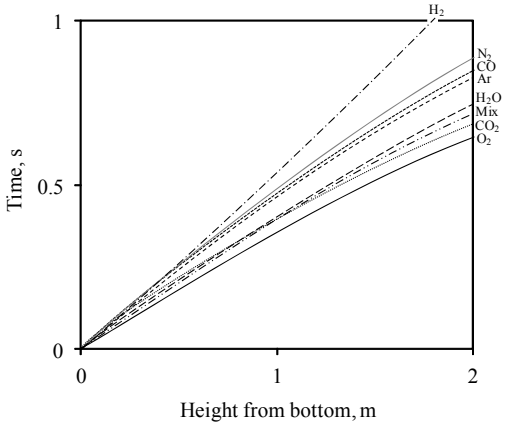

Fig.3. Residence time of eight types' of bubbles in the bath.

The variations in bubble radius are shown in Fig.4. After a bubble of 0.01 m radius is formed at the bath's bottom, the bubble is heated and rapidly expands as a result of thermal expansion. A transitory decrease in the radius of an O_2 bubble after the initial rapid increase is brought by thermal contraction due to the decrease in the bubble's temperature. The bubble size increases slowly later due to the loss of hydrostatic pressure. The changes in the number of moles of a bubble during its rising are different from one type of gas bubble to another, which also contributes to the size changes. The decrease in size

of the H_2 bubble after the thermal expansion is the result of the decreased number of moles. The sizes of eight injected bubbles arrived at the bath surface are in an order of CO_2, O_2, Mix, H_2O, Ar, CO, N_2, H_2.

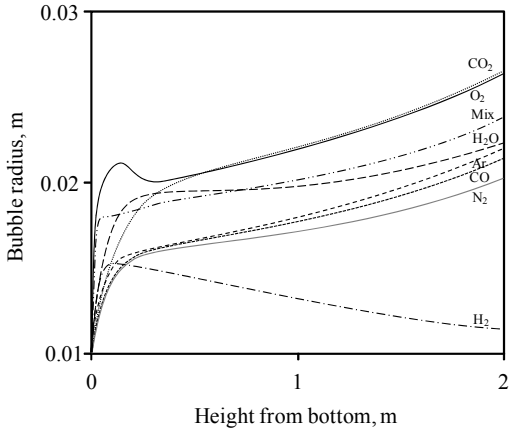

Fig.4. Radius of eight types' of bubbles in the bath.

The number of moles in an initial bubble was determined from the temperature, the radius and the pressure of the initial bubble at the bath's bottom. As seen in Fig.5, the number of moles of the bubble (n_g) changes due to reactions with the metal. For the O_2 bubble, n_g increases after a stagnant period. The stagnancy occurs because O_2 in the bubble is replaced with CO_2 of the same number of moles through a reaction of $O_2+\underline{C}=CO_2$. After the stagnancy, n_g increases due to the replacement of CO_2 with CO of about twice the number of moles through the reaction of $CO_2+\underline{C}=2CO$. For the CO_2 bubble, n_g increases from the beginning by the reaction of $CO_2+\underline{C}=2CO$. Desorption of nitrogen by $2\underline{N}=N_2$ and hydrogen by $2\underline{H}=H_2$ at the bubble's surface also contributes to the increase of n_g in O_2 and CO_2 bubbles. There is no significant change in n_g in the CO bubble during rising because the decrease of CO through $CO=\underline{C}+\underline{O}$ is counterbalanced by the increase of nitrogen and hydrogen through desorption at the bubble surface. n_g in the Ar bubble increases by the CO produced from $\underline{C}+\underline{O}=CO$ and also by desorption of nitrogen and hydrogen from the metal. As for the H_2O bubble, n_g initially increases by the reaction of $H_2O+\underline{C}=H_2+CO$ that produces twice as much gas than consumed. However, after a peak, n_g decreases by the absorption of hydrogen. For the H_2 bubble, n_g simply decreases by the absorption of hydrogen that overwhelms nitrogen desorption, plus the CO generation at the bubble surface. n_g in the Mixed gas bubble is firstly unchanged due to the reaction of $O_2+\underline{C}=CO_2$ that produces the same amount of gas as that consumed. It then increases by the reactions of $CO_2+\underline{C}=2CO$ and $H_2O+\underline{C}=H_2+CO$ which produce more gas than that consumed. After a peak, it slightly decreases because of the absorption of nitrogen and hydrogen.

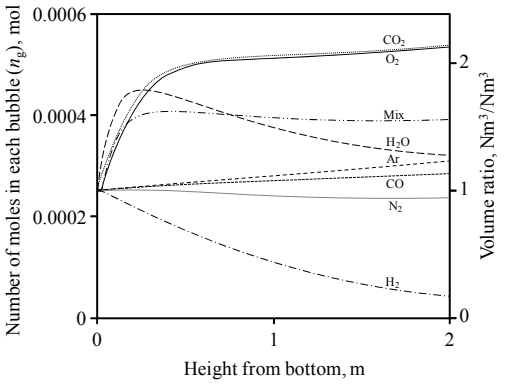

Fig.5. Number of moles of eight types' of bubbles in the bath. The right hand side shows the volume scale ratio of gases in the bath to the injected gases from the bath bottom.

The scale at the right side of Fig.5 is the volume ratio of gases in the bath to the injected gases at the bath bottom. The volumes of process off gas generated from injecting one cubic meter of gases are those at the bath surface in Fig.5. The off gas generated from injecting O_2 or CO_2 is more than twice that supplied. Injecting CO, Ar, H_2O or Mixed gas generates more off gas than that supplied and injecting N_2 or H_2 generates less off gas than that supplied. Since the stirring power of the bubbles in the bath is increased by increasing the gas amount, the stirring power supplied to the bath by the eight gases is therefore suggested from Fig.5 to be in an order of CO_2, O_2, Mix, H_2O, Ar, CO, N_2, H_2.

The changes of gas composition are shown in Fig.6. In the O_2 bubble (Fig.6a), O_2 decreases rapidly to approach zero by $O_2=2\underline{O}$ and $O_2+2\underline{C}=2CO$ at the bubble surface and $O_2+2CO=2CO_2$ in the bubble. CO_2 increases as the result. Once O_2 becomes lower, CO_2 decreases and CO increases by $CO_2+\underline{C}=2CO$. N_2 and H_2 increase by desorption from the metal that reduce the fraction of CO in the gas in the later period of the O_2 bubble rising. Initially, the desorbed hydrogen reacts with O_2 and CO_2 to produce H_2O in the bubble by $O_2+2H_2=2H_2O$ or $CO_2+H_2=CO+H_2O$. After increasing to a peak, H_2O decreases by $H_2O+\underline{C}=H_2+CO$ to near zero. H_2 starts to increase after O_2 and CO_2 contents become lower in the bubble. In the CO_2 bubble (Fig.6b), CO_2 is replaced by CO through $CO_2=\underline{C}+2CO$; N_2 and H_2 increases by desorption from the metal. There is a small amount of H_2O produced from desorbed hydrogen through $CO_2+H_2= CO+H_2O$ when CO_2 is rich in the initial bubble; H_2O decreases later by $H_2O+\underline{C}=H_2+CO$ to near zero when CO_2 depletes. In the CO bubble (Fig.6c), the fraction of CO decreases due to the increases of N_2 and

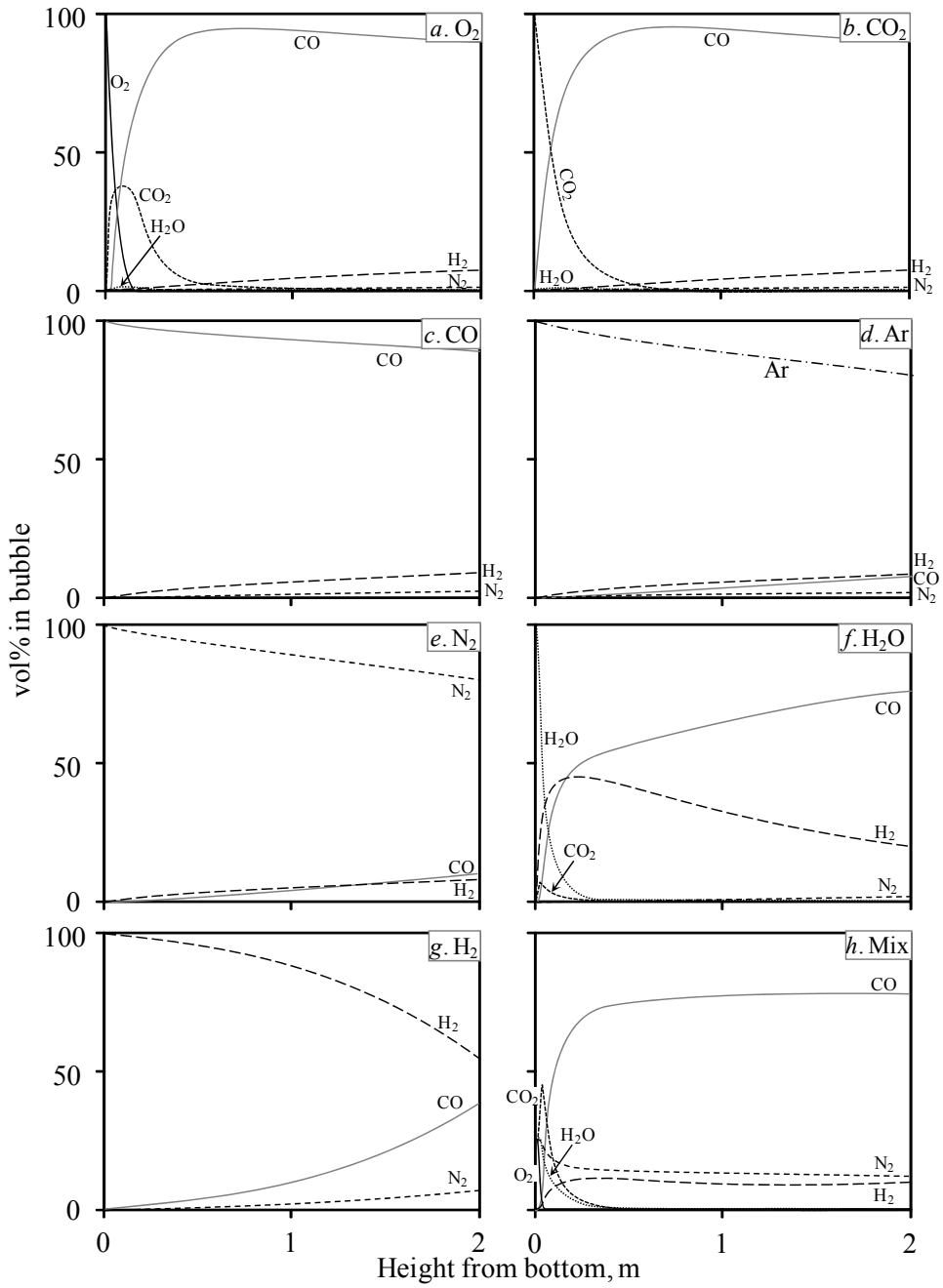

Fig.6. Compositions of the O_2 (*a*), CO_2 (*b*), CO (*c*), Ar (*d*), N_2 (*e*), H_2O (*f*), H_2 (*g*) and Mixed (*h*) bubbles in the bath.

H_2 by desorption. The decrease of CO is also due to the loss of CO in the bubble by the reaction of CO=C+O when the bubble is deeper in the bath, where pressure is high. In the Ar bubble (Fig.6d), CO pressure in the bubble is initially zero, which enables the reaction of C+O=CO to increase CO in the bubble. Meanwhile N_2 and H_2 increase in the bubble by desorption from the metal. The fraction of Ar in the bubble decreases as a result. In the N_2 bubble (Fig.6e), CO pressure in the bubble is also initially zero, which enables CO to be produced in the bubble; meanwhile N_2 decreases by absorption into the metal, and H_2 increases by desorption from the metal. In the H_2O bubble (Fig.6f), H_2O is replaced by H_2 and CO through H_2O+C=H_2+CO. H_2 decreases after a peak due to the loss of H_2 from the bubble by absorption. Since water gas shift reaction produces CO_2 when H_2O is rich in the initial bubble, CO_2 increases to a peak but soon decreases to near zero by CO_2 + C=CO.

Nitrogen desorption increases nitrogen in the bubble. In the H_2 bubble (Fig.6g), CO and N_2 increase by $\underline{C}+\underline{O}=CO$ and $2\underline{N}=N_2$ respectively which reduces the fraction of H_2 in the bubble. H_2 also decreases by the absorption into the metal. In the Mixed gas bubble (Fig.6h), O_2 in the bubble decreases rapidly to produce CO_2 by $O_2+\underline{C}=CO_2$. CO_2 increases as a result but it is in turn replaced by CO through $CO_2+\underline{C}=2CO$. After a short stagnant period, H_2O decreases by $H_2O+\underline{C}=H_2+CO$, which increases CO and H_2. Meanwhile, N_2 decrease due to absorption into the metal.

The composition of the process off gas is the composition of the bubbles that arrived at the bath surface in Fig.6. O_2, CO_2 and H_2O in the off gas are near zero. The off gases generated from O_2, CO_2 and CO injections are similar. Ar is rich in off gas generated from the Ar injection, N_2 is rich in off gas generated from N_2 injection and H_2 is rich in off gas generated from the H_2O and H_2 injections.

The oxygen content at various locations in the bath are shown by the ten lines in Fig.7. The [O] is the oxygen content in equilibrium with carbon in the bath under ambient pressure. $[O]_C$ marks the oxygen content in equilibrium with carbon in the metal under the local pressure; it decreases with increasing height from the bath bottom. $[O]_C$ equals [O] at the bath surface where the pressure is the ambient pressure. The other eight lines are oxygen content at the surfaces of the eight gas bubbles respectively; they vary with the depth of the bubbles.

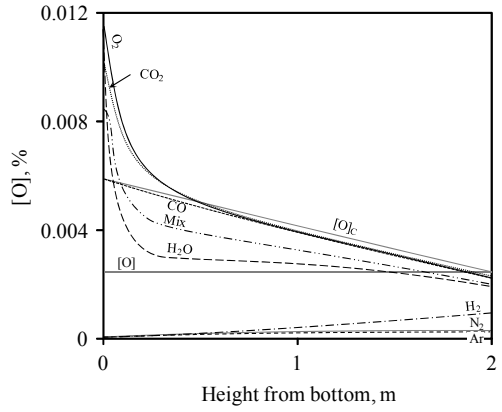

Fig.7. Oxygen content at the surface of eight types' of bubbles (O_2, CO_2, CO, Ar, N_2, H_2O, H_2, Mix), in the bath ([O]), and in equilibrium with carbon ($[O]_C$) in metal.

For O_2, CO_2, CO, H_2O or Mixed gas bubbles, the oxygen content at the bubble surface is initially high because either the bubble contains more oxidizing species such as O_2, CO_2 and H_2O, or the bubble is under higher pressure. As the bubbles rise in the bath, surface oxygen content decreases due to the loss of both oxidizing gases and pressure in the bubble. Oxygen is dissolved from these bubbles into the bath when the bubble is deep in the bath, because the surface oxygen of these bubbles is higher than [O]. However, oxygen is removed from the metal in to these bubbles when the bubbles rise to shallower locations in the bath because the surface oxygen of these bubbles close to the bath's surface becomes lower than [O]. The oxygen content at the surfaces of Ar, N_2 and H_2 bubbles are initially close to zero because there is no oxidizing gas in the three bubbles. The oxygen content at the surfaces of the three bubbles increases with increasing CO in the bubble. CO is produced by the reaction of $\underline{O}+\underline{C}=CO$ at the bubble surface; this reaction occurs because the oxygen content at the surface of three bubbles is lower than [O].

In production of high alloy steel using the bottom blown process, such as the production of stainless steel in AOD, gases of weak oxidization strength may be chosen to minimize the oxidation loss of the alloy element when decarburizing steel. The oxygen content at the bubble surface can be regarded as the oxidization strength of the bubble. As seen in Fig.7, the oxidization strength of O_2, CO_2, H_2O and Mix bubbles is rapidly lost as the bubbles move away from the bath's bottom, with strength loss particularly fast for the H_2O bubble. The oxidation loss of the alloy element is most likely to occur at the lower zone where the oxidization strength of the bubble is higher. The average oxygen content at bubble surface at 10 centimeters above the bath's bottom may be used to classify the oxidization strength of a bubble in a lower zone of the bath. Accordingly, the oxidization strength is suggested in the following order: O_2, CO_2, Mix, H_2O, CO, H_2, Ar and N_2.

The amounts of carbon, oxygen, nitrogen and hydrogen removed from the bath into the bubbles by blowing one cubic meter of a gas as a function of the height in the bath are shown in Fig.8. As seen in Fig.8(a), twice as much carbon is removed by O_2 injection as those by CO_2, H_2O or Mixed gas injection. Much less carbon is removed by injection of other gases. CO is unstable when it is deeper in the bath at a higher pressure because $[O]<[O]_C$. This brings small amounts of carbon pickup by the bath from CO injection due to the decomposition of CO. According to the total amounts of the removed carbon when the gas reaches the bath surface, the decarburization in the bath by the eight gases is suggested in the order of O_2, H_2O, Mix, CO_2, Ar, N_2, H_2 and CO. As seen in Fig.8(b), since oxygen content at the surface of O_2, CO_2, CO, H_2O and Mixed gas bubbles is higher than [O] when the bubbles are deeper in the bath, the oxygen dissolves from the gas into the metal. When Ar, N_2 and H_2 bubbles are injected into the bath, the oxygen is removed from bath to the bubbles as the result of lower oxygen content at the bubble's surface than in

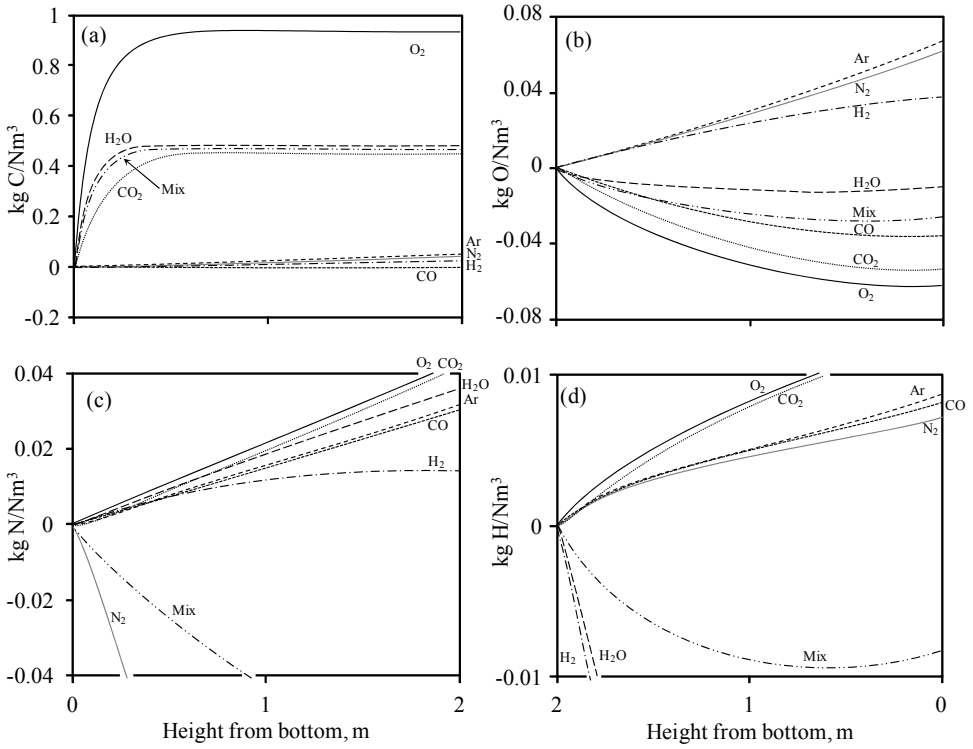

Fig.8. Carbon (a), oxygen (b), nitrogen (c) and hydrogen (d) removed from the bath by each cubic meter of eight types of gases.

the metal. According to the removed oxygen at the bath's surface, deoxidation by the eight types of gas is suggested in an order of Ar, N_2, H_2, H_2O, Mix, CO, CO_2, O_2. As seen in Fig.8(c), nitrogen is removed from metal into the gases that are free of N_2 in the initial bubbles. The amount of removed nitrogen was found to generally increase with increases in the volume of off gas (see Fig.5). There is more nitrogen removal by O_2 injection than by CO_2 injection because the size of an oxygen bubble is larger at the mid way point of rising in the bath (see Fig.4). For N_2 and Mixed gas bubbles that are initially rich in nitrogen, the bath absorbs the nitrogen. More nitrogen is absorbed from the N_2 bubble than from a Mixed gas bubble because nitrogen is richer in the former. Fig.8(c) suggests that denitrogenation of metal in the bath by eight types of gas is in an order of O_2, CO_2, H_2O, Ar, CO, H_2, Mix and N_2. Similarly, as seen in Fig.8(d), hydrogen is removed from metal into the gases that are free of H_2O or H_2 in the initial bubble and the removed amount also generally increases with increasing the volume of off gas. Hydrogen absorption occurs from injecting H_2O, H_2 and Mixed gas bubbles. Dehydrogenation was suggested to be in an order of O_2, CO_2, Ar, CO, N_2, Mix, H_2O and H_2.

Heat supplied from a bubble to the metal is shown in Fig.9. For an O_2 bubble, after a short stagnant period

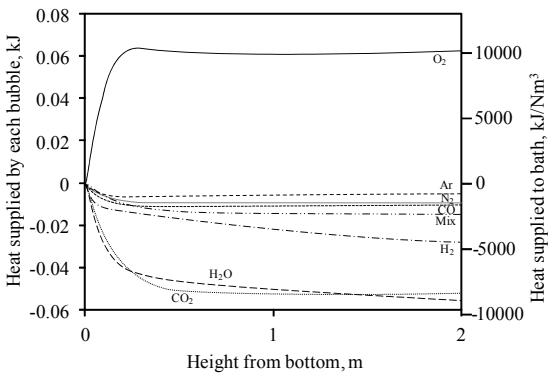

Fig.9. Heat supplied from each bubble of the eight types of gases to the metal at a given height from the bath bottom. The right hand side shows the heat scale supplied to the bath by each cubic meter of injected gases.

during the heat exchange with the initially cold bubble, the heat rapidly increases by the exothermic reactions of $O_2+2\underline{C}=2CO$ and $O_2+2CO=2CO_2$. Then the heat decreases by the endothermic reaction of $CO_2+\underline{C}=2CO$. For a CO_2 bubble, the heat is negative because of the heat required by the endothermic reaction of $CO_2+\underline{C}=2CO$ and by heating the initially cold bubble. For the CO bubble, the heat is negative because of the heat absorption

by the endothermic reaction of CO=C+O and by heating the initially cold bubble. For an Ar bubble, the negative heat is the result of less heat supplied from the exothermic reaction of C+O=CO at the bubble surface as compared to the heat lost by heating the initially cold bubble. The thermal effect of a N_2 bubble is similar as that of an Ar bubble but there is additional heat loss to nitrogen absorption. For a H_2O bubble, the heat is absorbed by the endothermic reaction of H_2O+C=H_2+CO and by heating the initially cold bubble. The thermal effect of a H_2 bubble is also similar to that of an Ar bubble, but there is additional heat loss due to hydrogen absorption. For a Mixed gas bubble, the heat slowly decreases initially and then decreases faster. This is the combined result of the exothermic reactions of O_2+2C=2CO and O_2+2CO=2CO_2 in the earlier period, and the endothermic reactions of CO_2+C=2CO, H_2O+C=H_2+CO, N_2=2N and H_2=2H in the later period in addition to the heat required for increasing sensible heat in the bubble in the earlier period. The heat in kilojoules supplied to the bath by each cubic meter of injected gas is shown by the scale at the right side of Fig.9. When gases arrive at the bath's surface, the bath receives heat from injecting O_2 but loses the heat when injecting the other seven. The amount of heat supplied to the bath by eight gases is in an order of O_2, Ar, N_2, CO, Mix, H_2, CO_2 and H_2O.

The bubble temperature is shown in Fig.10. The O_2 bubble is heated by the surrounding metal, and by the exothermic reactions at the surface of and in the bubble. Its temperature increases from 200°C to a temperature much higher than the bath temperature and then decreases to the bath temperature. This temperature decrease is responsible for the transitory contraction of the O_2 bubble in Fig.4. A similar temperature variation also appears to affect the Mixed gas bubble. Without the heat supply from the secondary combustion reaction (7), the temperatures of the other six bubbles do not increase to a temperature above the bath. The temperature of H_2 bubble is closest to the bath temperature because the thermal conductivity of H_2 is much larger than others.[21] The average temperatures of O_2 and Mixed gas bubbles within 10 centimeters above the bath's bottom are higher than the bath, but the others are lower than the bath. The average temperatures are in an order of O_2, Mix, H_2, Ar, H_2O, CO, N_2 and CO_2. For all the bubbles, however, their temperatures are the same as the bath's temperature when the bubbles leave the top surface of the bath as off gas.

Based on the temperature in Fig.10 and the composition in Fig.6 at the bath surface, and considering CO and H_2 in the gas as fuel, the calorific values of the off gas were estimated from the sensible heat plus the fuel calorific value. They are in an order of CO_2, O_2, CO, H_2O, Mix, H_2, N_2, Ar. There is twice as much off gas as that injected for O_2 or CO_2 injections (see Fig.5), the thermal energy lost in the off gas would be significantly higher for these two gases.

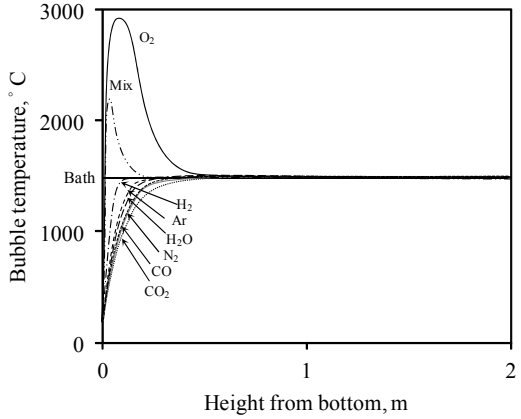

Fig.10. Temperatures of eight types of bubbles in the bath.

The rate of heat supply by a gas bubble can be obtained from the slopes of curves in Fig.9 and time-height relations in Fig.3. To represent the heat intensities at the lower zone of the bath, it is further converted to the averages of the rates of the heat supplied by each cubic meter of injected gas within 10 centimeters above the bath bottom. The O_2 bubble was found to supply heat to the metal at a significantly higher rate near the bath's bottom which enhances the erosion of the bottom refractory. The other seven gases absorb heat to lower the local temperature at the bath's bottom, which protects the bottom refractory. The gases that absorb heat faster are more suitable as coolant; hence the cooling effects of the eight gases were found to be in an order of H_2O, CO_2, H_2, Mix, CO, N_2, Ar, O_2.

6. CONCLUSIONS

Material and thermal effects of injecting O_2, CO_2, CO, Ar, N_2, H_2O, H_2 and a Mix of (25%O_2-25%CO_2-25%N_2-25%H_2O) gases in steel were simulated and compared by a model developed in this study that couples the rates and thermal effects of reactions, mass transport and heat transport between metal and gas bubbles. The results of a gas bubble of 0.01 m radius at 200°C injected into a bath of Fe-3C-0.0025O-0.005N-0.005S-0.0005H (in mass%), with a 2 m depth, at 1500 °C and under ambient pressure show that, the eight gases used in the bottom blown process are in the orders of (1) H_2, N_2, CO, Ar, H_2O, Mix, CO_2, O_2 for the bubble life in the bath; (2) CO_2, O_2, Mix, H_2O, Ar, CO, N_2, H_2 for the bubble size at the bath surface, amount of off gas and the stirring power; (3) O_2, CO_2, Mix, H_2O, H_2, Ar, N_2 for the oxidizing strength of the gas at the lower bath zone; (4) O_2, H_2O, Mix, CO_2, Ar, N_2, H_2, CO for decarburization;

(5) Ar, N_2, H_2, H_2O, Mix, CO, CO_2, O_2 for deoxidation; (6) O_2, CO_2, H_2O, Ar, CO, H_2, Mix, N_2 for denitrogenation; (7) O_2, CO_2, Ar, CO, N_2, Mix, H_2O, H_2 for dehydrogenization; (8) O_2, Ar, N_2, CO, Mix, H_2, CO_2, H_2O for the heat supplied to the bath; (9) O_2, Mix, H_2, Ar, H_2O, CO, N_2, CO_2 for gas temperature at the lower bath zone; (10) CO_2, O_2, CO, H_2O, Mix, H_2, N_2, Ar for calorific value in off gas; and (11) H_2O, CO_2, H_2, Mix, CO, N_2, Ar, O_2 for the cooling effect at the lower bath zone.

SYMBOLS

A: Surface area of a bubble, m^2
C_{pi}: Thermal capacity of i in gas, J/mol K
c_i: Content of i in gas or metal, mol/m^3
c_i^*: Content of i at bubble surface, mol/m^3
H_j: Enthalpy of j, J/mol
h_g: Heat transfer coefficient in gas, J/K m^2s
h_m: Heat transfer coefficient in metal, J/K m^2s
J_i: Mass transfer rates of i in gas or metal, mol/m^2s
k_i: Mass transfer coefficient of i in gas or metal, m/s
n_g: Number of moles of gas, mol
n_i: Number of moles of i in gas, mol
q_i: Heat generation rate by reaction (i), J/s
S_i: Generation rates of i by secondary combustion reaction, mol/m^3s
T_g: Temperature within bubble, K or °C
T_m: Temperature in metal, K or °C
T_s: Temperature at bubble surface, K or °C
t: Time, s
V: Bubble volume, m^3
W_i: Generation rates of i by water gas shift reaction, mol/m^3s

REFERENCES

1. M. Iguchi, T. Chihara, N. Takanashi, Y. Ogawa, N. Tokumitsu and Z. Morita: 'X-ray Fluoroscopic Observation of Bubble Characteristics in a Molten Iron Bath', *ISIJ Int.*, 1995, vol. 35, pp. 1354-1361.
2. K. Mori, M. Sano and H. Hoshino: 'Rate of Degassing from Molten Metal by Inert Gas Flushing', *Tetsu-to-Hagané,* 1975, vol. 61, pp. 182-194.
3. S.-M. Han, J.-H. Park, S.-M. Jung, J.-H. Park and D.-J. Min: 'Kinetic Study on Surface Dissolution of Nitrogen on Liquid Steel by Isotope Exchange Technique', *ISIJ Int*, 2009, vol. 49(2009), pp. 487-494.
4. W. Duan, H. Fukatsu, T. Nakatsukasa, M. Hirasawa and M. Sano: 'Reaction Kinetics of Dehydrogenation from Molten Iron under Inert Gas Atmosphere', *Tetsu-to-Hagané,*1996, vol. 82, pp. 905-910.
5. H. Sun and R. D. Pehlke: 'Kinetics of Oxidation of Multicomponent Liquid Iron Alloy by Oxidizing Gases Using Levitation Melting', *Transactions of the American Foundrymen's Society*, 1992, vol. 100, pp. 371-376.
6. H. Sun and R. D. Pehlke: 'Kinetics of Oxidation of Carbon in Liquid Iron-Carbon-Silicon-Manganese-Sulfur Alloys by Carbon Dioxide in Nitrogen', *Metall. Mater. Trans. B,* 1995, vol. 26, pp. 335-344.
7. H. Sun and R. D. Pehlke: 'Modeling and Experimental Study of Gaseous Oxidation of Liquid Iron Alloys', *Metall. Mater. Trans. B*, 1996, vol. 27, pp. 854-864.
8. H. Sun, K. Gao, V. Sahajwalla, K. Mori and R. D. Pehlke: 'Kinetics of Gas Oxidation of Liquid Fe-C-S Alloys and Carbon Boil Phenomenon'. *ISIJ Int.*, 1999, vol. 39, pp. 1125-1133.
9. H. Tokunaga, M. Iguchi and H. Tatemichi: 'Heat Transfer between Bubbles and Molten Wood's Metal', *ISIJ Int.*, 1995, vol. 35, pp. 21-25.
10. S. V. Komarov and M. Sano: 'Bubble Behavior and Heat Transfer in Preheated Gas Injection into Liquid Bath', *ISIJ Int.*, 1998, vol. 38, pp. 1045-1052.
11. H. Sun, Y.-C. Liu and M.-J. Lu: 'Physical, Chemical and Thermal Histories of an Oxygen Bubble in Bath during Bottom Blown Process', *Ironmaking Steelmaking*, 2016, vol. 43, pp. 697-704.
12. ISIJ: '*Iron and steel handbook, I: ironmaking and steelmaking*', ISIJ, ed. Maruzen, Tokyo, 3rd ed.; 1981, pp. 14-18.
13. W. Li: '*Physical chemistry of metallurgy and materials*', Chap. 1, '*Introduction to inorganic thermochemical database*', Beijing, Metallurgical Industry Publisher, 2001.
14. Q. Ma: '*Refining fundamentals*', Chap. 5, '*Thermal effect of metallurgical process*', 2004, Beijing, Metallurgical Industry Publisher, pp. 272-279.
15. R. Higbie: 'The rate of absorption of a pure gas into a still liquid during short periods of exposure', *Trans. Am. Inst. Chem. Eng.*, 1935, vol. 31, pp. 365-383.
16. J. Happel and H. Brenner: '*Low Reynolds number hydrodynamics*', The Hague/Boston/Lancaster, Martinus Nijhoff Publishers; 1983, pp.125-129.
17. F. Heisterkamp and K. Lohberg: 'Diffusion of carbon into liquid iron-carbon-silicon', *Arch. Eisenhüttenwes.*, 1960, vol. 37, pp. 813-819.
18. J. O. Hirschfelder, C. F. Curtiss and R. B. Bird: '*Molecular theory of gasses and liquids*', New York, Wiley, 1954, pp. 123-140.
19. Y. Kawai and Y. Shiraishi: '*Handbook of physico-chemical properties at high temperatures*', Tokyo, ISIJ., 1988, pp. 321-330.
20. Japan Society for Promotion of Science and Technology, 19th Committee of Steel Making: '*Recommended Equilibrium Value of Steel-Making*', Tokyo, 1984.
21. X. Zhang: '*Transport Theory in Metallurgy*', Beijing, Metallurgical Industry Publisher, 1988, pp. 430-439. □